Cement and Concrete Research 40 (2010) 128–136

Contents lists available at ScienceDirect

Cement and Concrete Research

journal homepage: http://ees.elsevier.com/CEMCON/default.asp

Thermal properties of hydrating calcium aluminate cement pastes

Neven Ukrainczyk *, Tomislav Matusinović

Faculty of Chemical Engineering and Technology, University of Zagreb, Marulićev trg 20, HR-10 000 Zagreb, Croatia

ARTICLE INFO

Article history:
Received 4 May 2009
Accepted 9 September 2009

Keywords:
Calcium aluminate cement
Hydration
Thermal properties
Transient hot wire method
Inverse problem

ABSTRACT

As the hydration of calcium aluminate cements (CAC) is highly temperature dependent, yielding morphologically and structurally different hydration products that continuously alter material properties, a good knowledge of thermal properties at early stages of hydration is essential. Thermal diffusivity and thermal conductivity during CAC hydration was investigated by a transient method with a numerical approach and a transient hot wire method, respectively. For hydration at 15 °C (formation of mainly CAH_{10}), thermal diffusivity shows a linear decrease as a function of hydration degree, while for hydration at 30 °C there is a linear increase of thermal diffusivity. Converted materials exhibited the highest values of thermal diffusivities. The results on sealed converted material indicated that thermal conductivity increased with an increase in temperature (20–80 °C), while thermal diffusivities marginally decreased with temperature. The Hashin–Shtrikman boundary conditions and a simple law of mixtures were successfully applied for estimating thermal conductivity and heat capacity, respectively, of fresh cement pastes.

1. Introduction

Calcium aluminate cement (CAC) is a versatile special cement that is used in high performance applications [1–5] such as those requiring: resistance to chemical attack, high early strength, refractory, resistance to abrasion, and/or low ambient temperature placement. Data on thermal properties of CAC are particularly interesting due to high rate of heat generation in reaction of hydration and resulting high temperature gradient in material. During the hydration of CAC a large quantity, typically 70–90% of total heat is liberated in a short period (first 24 h) [4] that cause a considerable increase in material temperature, even above 100 °C. Setting and hardening of CAC is primarily due to the hydration of CA (cement notation: C=CaO, A=Al_2O_3, F=Fe_2O_3, S=SiO_2, H=H_2O), but other compounds also participate in the hardening process especially in long term strength development [3]. The hydration of CAC is highly temperature dependent [1–4], yielding CAH_{10} as main products at temperatures less than 20 °C, C_2AH_8 and AH_3 at about 30 °C, and C_3AH_6 and AH_3 at temperatures greater than 55 °C. CAH_{10} and C_2AH_8 [6] are known to be metastable at ambient temperature and convert to the more stable C_3AH_6 and AH_3 [7] with consequent material porosity and permeability increase and loss of strength. The conversion is accelerated by temperature and moisture availability. In the absence of sufficient water these phases do not convert but dehydrate [6,7]. In order to predict the course of hydration, the development of hydration products and prevent cracks due to thermal stresses, a good understanding of the thermal behavior of the material during hydration is required.

Measurements of thermal properties of cement materials as heterogeneous, wet and porous materials by conventional steady-state methods can produce large errors. In order to avoid water migration during the long run-time of the steady thermal tests, transient measurement methods are preferable [8,9]. The determination of thermal diffusivity and thermal conductivity is very challenging since it belongs to a class of inverse problems where an estimated parameter is very sensitive to measured quantities necessary for its calculation.

Data on the thermal conductivity, diffusivity and specific heat of hydrating CAC pastes are scarce and insufficient. Even the published values for thermal properties on hydration of PC still show high scatter and results can be contradictory [10–12]. On hydrated CAC paste (w/c = 0.45, cured for one week at 80 °C and 20 MPa) Espinosa-Paredes et al. [13,14] documented surprisingly low thermal conductivity and specific heat, and higher thermal diffusivity in comparison to PC. They used the parallel wire method which is very sensitive to the measured radial distance of a thermocouple from a heater. Unfortunately, in that study the type of CAC used was not specified and the moisture conditions were not controlled. Santos [15] studied the effect of moisture and porosity on thermal conductivity, diffusivity and specific heat on a conventional aluminous refractory concrete (low-iron CAC). Kim et al. [16] reported that thermal conductivity of Portland cement pastes decreases linearly with increasing curing temperature. However, the information on the influence of temperature on the thermal properties of hydrated cement pastes appears to be scarce. Espinosa-Paredes et al. [13,14] investigated thermal conductivity and diffusivity and specific heat capacity of Mexican cementing systems used in geothermal well completion in the temperature range 28 to 200 °C based on a parallel wire technique. Mounanga et al. [17] measured thermal conductivity evolution on hydrated PC paste (w/c = 0.348) by a parallel wire method.

* Corresponding author. Tel.: +385 1 4597 228; fax: +385 1 4597 250.
E-mail address: nukrainc@fkit.hr (N. Ukrainczyk).

0008-8846/$ – see front matter © 2009 Elsevier Ltd. All rights reserved.
doi:10.1016/j.cemconres.2009.09.005

Authors applied temperature corrections by assuming pure additive effect between the heat generated by hydration reactions and the one supplied by the electric current. Consequently, the temperature rise due to the hydration heat ($\Delta T \sim 60$ °C) was straightforwardly subtracted from the wire temperature increase. At maximal rate of hydration, hydration degree of about 30%, and temperature of about 85 °C, Mounanga et al. [17] documented 40% and 36% higher thermal conductivity than that of a fresh cement paste and hardened paste (degree of hydration, $\alpha \sim 0.55$), respectively. On the other hand, Bentz [12] documented by applying transient plane source measurement technique on small semi-isothermal (twin) specimens, a little variation in thermal conductivity with degree of hydration.

In view of the lack of data, a specially designed experimental program dealing with the determination of thermal properties of fresh iron-reach CAC pastes and morphologically different hydrated CAC material had been conducted. Also, influence of temperature on thermal diffusivity and conductivity of hydrated material had been investigated.

2. Theoretical

Thermal diffusivity a ($m^2\ s^{-1}$) is an important property of material in all problems involving transient heat conduction. It is a measure of rapidity of the heat propagation through a material and combines thermal conductivity (λ), specific heat (c_p) and density (ρ) according to:

$$a = \frac{\lambda}{\rho c_p} \tag{1}$$

Cement based material is a complex heterogeneous, multiphase and polydisperse system. Through such a material the heat is transferred by a combination of different modes, including conduction through the solid particles, conduction and convection through the gaseous and liquid phases, evaporation — condensation mechanism [9,17], and radiation at the particle surfaces. In evaporation — condensation mechanism water evaporates from the pore warm surface, and then migrates by gaseous diffusion process and condensates on the cold surfaces, thus transferring its latent heat of vaporization. However, the overall heat transfer process is practically modelled solely by a heat conduction model considering the conduction parameters as apparent. Therefore, one should bear in mind that the physical parameters measured in this paper are more properly called apparent thermal conductivity and apparent thermal diffusivity. Transient heat conduction in the radial direction in an infinite cylinder, considering temperature independent thermal properties, can be expressed as [18]:

$$\frac{1}{a}\frac{\partial T}{\partial t} = \frac{\partial^2 T}{\partial r^2} + \frac{1}{r}\frac{\partial T}{\partial r} + \frac{q_v}{\lambda} \tag{2}$$

where q_v is a volumetric heat generation term (W/m^3).

2.1. Hot wire model

When heat is generated into the line source immersed in the sample, its temperature response is based on an analytical solution [18] to the heat conduction model given in cylindrical coordinates:

$$\Delta T(r_w, t)_{t=0}^{t=t} = \frac{P}{4\pi\lambda}\left[-E_i\cdot\left(-\frac{r_w^2}{4at}\right)\right] \tag{3}$$

where λ is the thermal conductivity of sample ($W\ m^{-1}K^{-1}$), r_w is the radius of the wire (m), a is thermal diffusivity of sample ($m^2\ s^{-1}$), t is time (s), P is rate of line heat generation ($W\ m^{-1}$) and E_i is the exponential integral computed as:

$$E_i(-z) = \gamma + \ln z + z - \frac{z^2}{2!} + \frac{z^3}{3!} - \frac{z^4}{4!} + \ldots.. \tag{4}$$

in which $\gamma = 0.5772156649...$ is Euler's constant and $z = r_w^2/(4at)$.

3. Experimental

3.1. Materials

This paper examines the hydration of sample of commercial CAC ISTRA 40 taken from a regular production of Istra Cement International, Pula, Croatia. The cement has the oxide mass fraction composition listed in Table 1. Physical properties of used cement are given in Table 2. The main compounds are CA and ferrite phase (C_4AF–C_6AF_2), with mayenite, $C_{12}A_7$, gehlenite, C_2AS and β-C_2S as minor compounds. The QXRD analysis of investigated CAC gave the mass proportions of CA and $C_{12}A_7$ to be 41% and 4%, respectively. All samples were prepared with deionized water.

3.2. Experimental setup

For thermal diffusivity and thermal conductivity specimens were prepared by casting in cylindrical copper containers with inner diameter $2R = 51$ or 26 mm, length 250 mm. The specimen geometry assured the one-dimensional heat transfer. Thickness of a larger ($2R = 51$ mm) and a smaller ($2R = 26$ mm) container, is 1 and 0.5 mm, respectively. The copper tube was carefully filled with the cement paste continuously applying vibrations in order to minimize air entrapment. The thermocouple or the hot wire was placed at the axis of the tube. The copper tube was carefully sealed with styropore and rubber stoppers and placed vertically in the temperature controlled water bath (±0.03 °C). The wires exit through the upper base of the tube which was above a bath water level, Fig. 1. Further details on experimental setup for the determination of thermal difusivity and thermal conductivity are described in Sections 3.4. and 3.5.

3.3. Experimental plan

In order to investigate thermal properties of fresh CAC pastes and morphologically different hydrated CAC material, the aimed specimens were obtained according to a designed experimental hydration program shown in Table 3. Specimens with water to cement mass ratio of 0.3 and 0.4 were prepared. All the transient thermal properties tests were conducted after and during a period of sufficiently constant rate of hydration to assure a stabilization of temperatures prior to excitement and eliminate heat generation term [19] in Eq. (2). Thermal diffusivity tests during period of low rate of hydration were conducted on specimens 51 mm in diameter. Thermal diffusivity tests during period of maximal rate of hydration were conducted on samples 26 mm in diameter. Specimens were tested after the defined hydration program in Table 3. The fresh pastes were tested at temperature 20 °C during the period of 1.5–2.5 h after mixing. Temperature change for the thermal diffusivity tests was $\Delta T \sim 5$ K for larger tube and $\Delta T \sim 3$ K for smaller tube. The specimens were hydrated at 14 or 30 °C to obtain CAH_{10} or C_2AH_8 and AH_3 as main hydration products, respectively. After 30 h hydration, the metastable hydrates were converted to stable C_3AH_6 and AH_3 by additional heating at 70 °C in a water bath for 24 h. Range of test

Table 1
Chemical composition of investigated CAC.

CaO	Al_2O_3	Fe_2O_3	FeO	SiO_2	TiO_2	MgO	SO_3	Na_2O	K_2O	Sum
37.10	38.47	14.39	2.90	4.43	1.05	0.90	0.20	0.14	0.17	99.8

Table 2
Physical properties of investigated CAC.

>90 μm, %	Blaine, cm^2/g	Specific gravity, g/cm^3	Setting time, min		Standard consistency, %	Bulk density, kg/m^3	
			Initial	Final		Loose	Compacted
3.76	3401	3.20	298	329	24.0	950	1776

temperatures of specimens is given in last two columns in Table 3. In order to test the influence of temperature on thermal diffusivity of converted CAC paste, a series of tests with temperature change $\Delta T \sim 5$ K were conducted on specimens Conv70C in temperature range 13–80 °C. Influence of temperature on thermal conductivity was investigated on specimens Conv70C at temperatures 20, 40, 60, and 80 °C. Tests were conducted after a temperature stabilization period of 2 h.

3.3.1. Air content of fresh cement pastes

The air content of the fresh cement pastes ($w/c = 0.3$ and 0.4) at 20 °C were determined by pressure method as described in standard EN 1015-7. For prepared fresh cement pastes with water to cement ratio 0.3 and 0.4 the measured air contents are 1.35% and 0.55% by vol., respectively. Measurements on repeated preparations (3 times) of the fresh cement pastes for $w/c = 0.3$ and 0.4 indicated an air content standard deviation of 0.10% and 0.05%, respectively (somewhat less than 10% relative change). All the fresh cement pastes were initially hydrated in the temperature range 15–30 °C (see Table 3). By applying Boyle–Mariott law (assuming a constant pressure) a 10 K change in temperature of fresh cement paste results in 3% relative change of the air content value.

3.4. Thermal diffusivity determination

3.4.1. Measurement setup

The experimental setup consisted of two constant-temperature water baths (±0.03 °C), the copper tube container, K-type thermocouples wiring, data acquisition unit and a PC. To determine thermal diffusivity of investigated specimens, an experimental transient method was used [19–21]. In this method a cylindrical specimen in copper tube

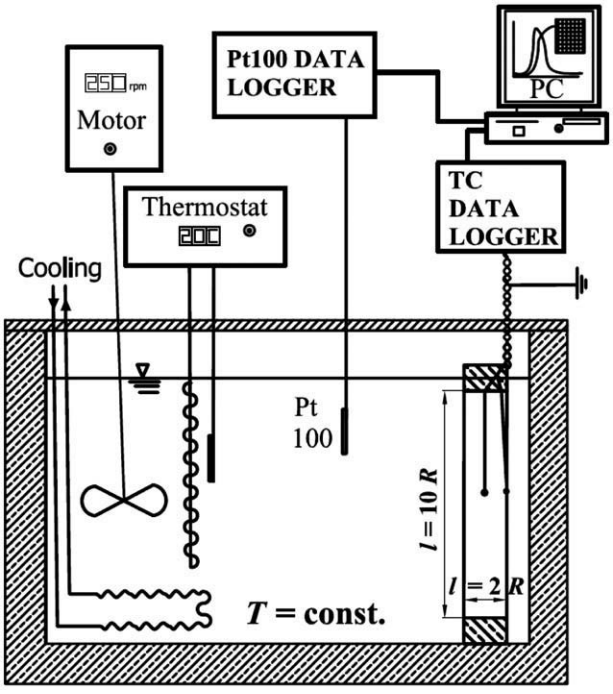

Fig. 1. Thermal diffusivity measuring apparatus.

Table 3
Experimental hydration program conducted in order to obtain thermal conductivity and evolution of thermal diffusivity during developing morphologically different hydration products.

Specimen label	Hydration program ($w/c = 0.3$ & 0.4)	Sample diameter, mm	Test temperature, °C	
			a	λ
Fresh	20 °C, 1.5 h	51	20–25	20
15CTmax	15 °C, tested during period of maximal rate of hydration	26	15–18	–
15C30h	15 °C for 30 h	51	13–30	20
30CTmax	30 °C, tested during period of maximal rate of hydration	26	30–27	–
30C30h	30 °C for 30 h	51	30–13	20
Conv70C	15 °C for 30 h, converted 24 h at 70 °C	51	13–80	20–80

container, attained a uniform temperature of the first bath, T_1 and then was suddenly immersed in the second bath at temperature $T_1 + \Delta T$. The temperature $T(r \sim 0, t)$ at the tube axis was measured as a function of time. Furthermore, the boundary temperature was measured at the inside surface of the copper tube wall. At the end of the series of experiments the sample was cut and an accurate radial position of the thermocouple measuring end was obtained and the sample was checked for the homogeneity. Good bond between hydrated material and copper container was observed on all specimens that provides a desirably good thermal contact.

K-type thermocouples 0.2 mm thick with grounded twisted-shielded wiring were used to obtain accuracy and eliminate noise. Cable shielding and twisted wire pairs were used to minimize or eliminate capacitive coupled interference and to aid in lowering electromagnetically induced errors. The thermocouples were calibrated before use (using Pt 100 with an overall accuracy ±0.03 °C), and they were observed to have an accuracy of ±0.1 °C in a temperature range of 0–90 °C. An 8 channel data logger (TC-08 Pico technology) was used for temperature measurements. The 20 bit resolution ensured detection of minute changes in temperature (practical temperature resolution is 0.01 °C). It was capable of storing the entire set of temperatures once every 100 ms. The experimental data is simultaneously transferred to a PC. Thermocouple cold junction is held at room temperature and sensed by a precision thermistor in good thermal contact with the input connectors on thermal block, all being an integral part of the TC-08 measuring instrument. In order to have an accurate cold junction compensation, its temperature change was kept as low as possible.

3.4.2. Numerical model for inverse thermal diffusivity estimation

Based on the experimental transient method described in Section 3.4.1 the thermal diffusivity of the sample can be estimated by fitting the experimental results to a theoretical expression based on a Bessel function [20] or its linear (first term) approximation [21]. In this work a numerical approach for thermal diffusivity estimation was adopted for better accuracy and precision. Instead of assuming an ideal step temperature excitement, a measured temperature for the boundary condition was employed. Fourier's one dimensional radial heat conduction model in Eq. (2) was solved using Matlab's built-in solver "pdepe" [22,23]. The heat generation term was neglected (please see Sections 3.3 and 4.2 for further discussion on this). The Levenberg–Marquardt method [24,25] for optimization was used for the solution of the inverse problem of the parameter estimation [26]. The inverse problem was solved and optimized by using a sub-program that was written [27] for the setting of Matlab 6.5 (The MathWorks, Inc., Natick, MA); script files comprising a specially built graphical user interface are freely available upon request to the corresponding author. Inputs for this numerical model were temperature–time arrays, i.e. $T(r = R, t)$ and $T(r \sim 0, t)$, along with the initial condition $T(r, t = 0) = \text{const}$. In order to speed up the iterative computing, the temperature–time input was

reduced as follows. First, the accurate onset of excitement was determined from raw temperature data collected each 100 ms. Then, the temperature records were reduced to about 1000 time points per measurement. The output of the numerical model gives a result of the thermal diffusivity estimate, as shown in Fig. 2.

The results of the method evaluation on reference materials indicated an accuracy of 1% and a precision of 0.7% (for 95% confidence) [27]. The reference materials used to evaluate the method and the apparatus were gelatinous water (Agar gel 0.7%), glycerol (p.a. redistilled) and Ottawa (quartz) sand.

3.5. Thermal conductivity determination

3.5.1. Measuring device

As the parallel wire method is very sensitive to the uncertainty of measuring the radial distance of a thermocouple from a heater, a resistance technique is employed. Furthermore, by this method, where the wire acts as both a heater and a resistance thermometer, the influence of local non-homogeneities of measured materials is minimized. The thermal conductivity is determined from the time dependant temperature rise of an electrically heated wire. The wire used is 99.99+ % platinum (Aldrich) with a diameter $2r_w = 76\ \mu m$ and length of $l_w = 176$ mm. It is desired to have a wire with as small a diameter as possible because the theory assumes a true line heat source. The wire is heated by placing a constant voltage across the Wheatstone bridge, as suggested by Glatzmaier and Ramirez [28]. The supplied voltage has an output range of 0–25 V and is stable to within $\pm 10\ \mu V$. Change in the wire electrical resistance is determined by measuring the unbalanced voltage of a precision Wheatstone bridge during heating period. This voltage is read by a computer via an 8 channel 10-bit A/D converter. Measuring apparatus is connected to the personal computer via RS232 protocol that provides the sampling rate of 15 ms. Specially designed programs provide control of the automatic measuring apparatus and easy usage. The core of the measuring apparatus is a microcontroller PIC 16F877 which was programmed in MPLab by a direct RISC instructions and ICD-2 programmer/debugger. From the previously obtained resistance versus temperature calibration (least-squares regression) of the used Pt wire the change of the temperature is deduced. The low temperature rise of hot wire, obtained by applying low input voltage, is desirable in terms of minimizing the effects of natural convection, radiation and gas evolution. On the other hand, higher voltage reduces the effect of noise and allow for a more accurate temperature measurement. In this work the applied voltage during 2 min gave a temperature rise of 5 °C.

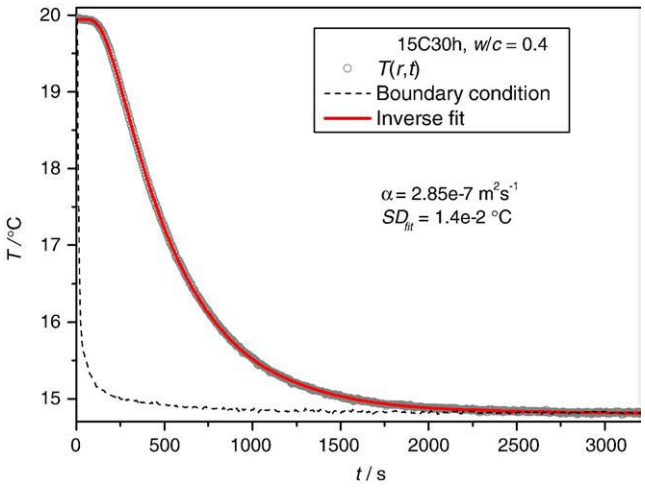

Fig. 2. An example of a result for estimation of thermal diffusivity based on the measured temperature response (specimen 15C30h) and the radial heat conduction model in Eq. (2).

The results of the method evaluation on reference materials indicated an accuracy of 3% and a precision of 0.7% (for 95% confidence) [29]. The reference materials used to evaluate the used apparatus and method are gelatinous water (Agar gel 0.7%), glycerol (p.a. redistilled) and Ottawa sand.

3.5.2. Experimental setup

The mould containing the cement paste is obtained in the same manner as for the thermal diffusivity experimental setup (in Section 3.4.1). A wire tensioning system is placed in the paste, the frame being next to the inside surface of the copper pipe. A thermocouple is placed about the tube axis to monitor the temperature of the sample. Once the paste has been cast, the mould is closed and sealed and put in the temperature controlled water bath.

3.5.3. Thermal conductivity estimation

Deviations from the idealized model in Eq. (3), classified as inner and outer, can be minimized by a proper selection of experimental conditions. Inner deviations arise from the non-ideality of the wire that has finite length, mass and heat capacity. These deviations, which depend on the properties of the wire, have significant impact only on the initial temperature response ($t < t_{min}$). Outer deviations are due to the finite dimensions of the sample and have impact at large times ($t > t_{max}$) when the outer boundary conditions (of the sample) influence the wire temperature response. The so-called time window, $t_{min} < t < t_{max}$ defines representative temperature response corresponding to thermal properties of investigated sample. By numerical simulation, supposing a systematic error of 0.1%, the time window is estimated to be between $t_{min} = 0.5$ s and $t_{max} = 120$ s. For simulations a numerical model of one dimensional radial heat conduction was built for the used experimental configuration and solved by using Matlab's built-in solver "pdepe" [22,23]. The model employed two coupled partial differential equations of energy conservation: one for the wire and one for the sample [30].

The thermal conductivity was obtained by fitting the experimental results to an analytic expression given by Eq. (3) by using previously obtained values for thermal diffusivity (in 3.4) and eight terms for calculating the value of exponential integral according to the Eq. (4). This parameter estimation problem was solved by the Levenberg–Marquardt method of optimization [24,25]. A simple parameter sensitivity analysis of the Eq. (3) indicates that an uncertainty of used value for thermal diffusivity has little impact to estimation of thermal conductivity [29].

3.5.4. Effect of cement paste electrical conductivity

The electrical conductivity of cement paste was measured by conductivity meter (Lab 960 Schott instruments) 1 h after mixing cement and water. For cement pastes with water to cement ratio 0.4 and 0.3 the measured electrical conductivities are 1287 μS cm^{-1} and 1098 μS cm^{-1}, respectively. The resistance of the cement paste sample in a defined geometry (in Section 3.2) is calculated by referring to the values of the obtained electrical conductivity. The deviation of the overall electrical resistance (of the parallel system of sample and Pt resistance wire), from the Pt resistance wire alone is calculated to be less than 0.5%. Hence, in the experimental configuration the systematic error due to the electrical conductivity of cement paste can be assumed to be less than 0.5%.

3.6. X-ray diffraction

The composition of CAC and hydrates formed was investigated by powder X-ray diffraction (XRD). Philips diffractometer PW1830 with Cu Kα radiation was used (the scan step was 0.01° with collection time of 2 s). The hydration was blocked and free water removed by addition of acetone (2-propanon). This was done by grinding the sample in three doses with acetone in agate mortar.

4. Results and discussion

4.1. XRD

XRD analysis on samples obtained from hydrated specimens cured at appropriate temperature confirmed the hydrate compositions expected from the literature [1–4]. The main hydrate observed on specimens 15CTmax and 15C30h was CAH_{10} with barely detectable quantity of C_2AH_8 and AH_3. Hydrates composition of 30CTmax and 30C30h is mainly C_2AH_8 and AH_3 with traces of CAH_{10} and C_3AH_6, respectively. Converted samples gave C_3AH_6 and AH_3 as hydrated products. Main diffraction peaks of metastable hydrates are fairly broadened, indicating poor crystallinity, while that of the stable hydrated material showed good crystallinity.

4.2. Thermal properties

As mentioned earlier, all the transient thermal properties tests were conducted after and during a period of sufficiently constant rate of hydration, controlled by monitoring the temperature measurement. During 1.5–2.5 h and after 30 h of hydration, rate of hydration exhibit a constantly low value with a heat generation of about 1 $Jh^{-1}g^{-1}$ [31]. This assured a constant heat generation term in Eq. (2) that provided a stabilization of temperatures prior to excitement and made accurate determination of thermal properties [19]. Thermal diffusivity and thermal conductivity tests during period of low rate of hydration were conducted on specimens 51 mm in diameter.

4.2.1. Thermal diffusivity

An example of a result for estimation of thermal diffusivity based on the measured temperature response (specimen 15C30h) and the radial heat conduction model in Eq. (2) is given in Fig. 2. A good fit with a standard deviation $SD_{fit} \sim 1.4 \cdot 10^{-2}$ K validates the heat conduction model used for describing the heat transfer of investigated wet porous materials.

Experimental results of thermal diffusivity are given in Table 4. The value obtained on fresh cement paste for w/c of 0.3 is 11% higher than for w/c of 0.4. The influence of composition of hydrated material on thermal diffusivity is as follows. The specimens composed of CAH_{10} (15C30h, $w/c = 0.3$ and 0.4) have the lowest values of thermal diffusivity, even below the value of fresh cement pastes. Converted materials (Conv70C) exhibit the highest values of thermal diffusivities. For the sake of comparison on available literature data, it is worth noting that Hansen et al. [32] documented an increase of thermal diffusivity during hydration of rapid hardening portland cement, $w/c = 0.5$ at $T = 30$ °C, from about $2.36 \cdot 10^{-7}$ to $2.92 \cdot 10^{-7}$ m^2/s, which is consistent (a lower value for a higher water content) with the data obtained in this paper.

4.2.2. Thermal conductivity

An example of a result for estimation of thermal conductivity based on the measured temperature response (specimen Conv70C $w/c = 0.4$) and the radial heat conduction model in Eq. (3) is given in Fig. 3. A good fit with a standard deviation $SD_{fit} \sim 1.9 \cdot 10^{-2}$ K validates the application

Table 4
Experimental and calculated results of thermal properties at $T = 20$–25 °C. Specific heat capacities are calculated upon Eq. (1).

Specimen label	λ/W(m K)$^{-1}$		a 10^7/m^2 s^{-1}		c_p/J(g K)$^{-1}$	
	w/c 0.4	w/c 0.3	w/c 0.4	w/c 0.3	w/c 0.4	w/c 0.3
PasteFresh	0.98	1.06	2.97	3.30	1.69	1.52
15CTmax	–	–	2.93	3.25	–	–
15C30h	0.97	1.06	2.85	3.19	1.74	1.57
30CTmax	–	–	3.02	3.40	–	–
30C30h	0.96	1.05	3.12	3.55	1.57	1.40
Conv70C	0.96	1.05	3.40	3.82	1.44	1.30

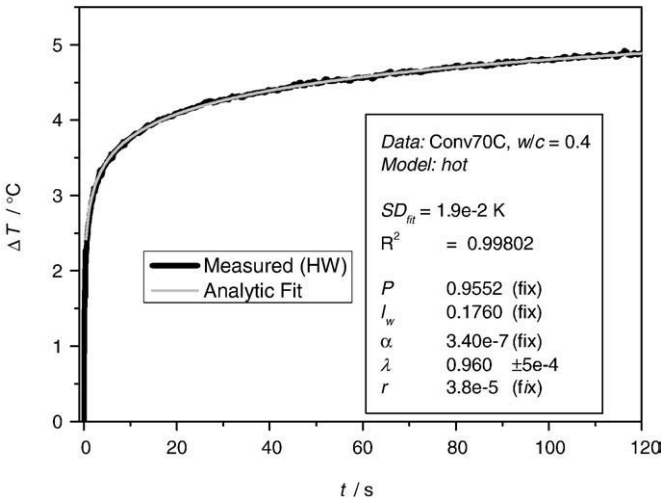

Fig. 3. An example of a result for determination of thermal conductivity based on a measured temperature response (Conv70C $w/c = 0.4$) and the heat conduction model in Eq. (3).

of the heat conduction model used for describing the heat transfer of the investigated wet and porous materials.

Experimental results of thermal conductivity are given in Table 4. The value obtained on fresh cement paste for $w/c = 0.3$ is 8% higher in comparison to $w/c = 0.4$. Fresh cement pastes have the highest thermal conductivities, in exception of the specimen 15C30h $w/c = 0.3$ which has same the value as the corresponding fresh paste. Hydrated materials cured at 30 °C and converted materials with $w/c = 0.3$ and 0.4 exhibit lower values of thermal conductivity than cement fresh paste of about 1% and 2%, respectively. The values of the thermal conductivity for fresh calcium aluminate cement pastes obtained show reasonable agreement with the available literature values for Portland cement reported by Bentz [12], 0.97 W $m^{-1}K^{-1}$ and 0.99 W $m^{-1}K^{-1}$ for w/c of 0.4 and 0.3, respectively, and especially by Mounanga et al. [17] for $w/c = 0.348$ of 1.0 W $m^{-1}K^{-1}$. Hansen et al. [31] documented a decrease of thermal conductivity (0.88 W $m^{-1}K^{-1}$ at early ages to 0.78 W $m^{-1}K^{-1}$ at later ages) during hydration of rapid hardening portland cement, $w/c = 0.5$ at $T = 30$ °C, while Mounanga et al. [17] obtained an increase.

Thermal conductivity of the fresh cement paste is modeled by Hashin and Shtrickman (HS) model. The upper (λ_u) and lower (λ_l) HS bounds for the thermal conductivity of the multi-phase composite, λ_{mp} are [12,17,33]:

$$\lambda_A + \frac{B_A}{1 - \frac{B_A}{3\lambda_A}} \le \lambda_{mp} \le \lambda_C + \frac{B_C}{1 - \frac{B_C}{3\lambda_C}} \tag{5}$$

where for the three components: air (A), liquid water (H) and cement (C):

$$B_A = \frac{\Phi_H}{\frac{1}{\lambda_H - \lambda_A} + \frac{1}{3\lambda_A}} + \frac{\Phi_C}{\frac{1}{\lambda_C - \lambda_A} + \frac{1}{3\lambda_A}}; \quad B_C = \frac{\Phi_H}{\frac{1}{\lambda_H - \lambda_C} + \frac{1}{3\lambda_C}} + \frac{\Phi_A}{\frac{1}{\lambda_A - \lambda_C} + \frac{1}{3\lambda_C}} \tag{6}$$

where φ_i is a volume fraction of the component i, λ_H is the thermal conductivity of liquid water [34] (0.604 W $m^{-1}K^{-1}$ at 20 °C), λ_C thermal conductivity of the cement component and λ_A thermal conductivity of the air component (0.025 W $m^{-1}K^{-1}$ [17]). For λ_C, Mounanga et al. [17] used the reported value on crushed hydrated cement paste ($\lambda_C = 2.85$ W $m^{-1}K^{-1}$). Bentz [12] used two component (2 K) HS model, $\varphi_A = 0$ in Eq. (6), (the air content was not measured in the study) to estimate the thermal conductivity of the cement component, and reported the value $\lambda_C = 1.55$ W $m^{-1}K^{-1}$, from the measured thermal conductivities of the fresh portland cement pastes. In this work the value for the thermal conductivity of the CAC component was estimated in a manner to provide the HS bonds that encompass

both of the experimental values for the fresh pastes with $w/c=0.3$ and 0.4 given in Table 4. Results of the estimation gave $\lambda_C=2.13$ W m^{-1}K^{-1} and $\lambda_C=1.68$ W m^{-1}K^{-1} for the used three component, 3K-HS model (Eq. (5) and (6)) and the 2K-HS, respectively.

The 2K-HS model assumes the influence of the air content through the apparent value of λ_C, which is lower than the true value. It should be noted that such simplified model doesn't consider the change of the air content with the w/c ratio. Calculated values for thermal conductivity of the fresh cement pastes based on 3K-HS model are λ_l ($w/c=0.3$) = 0.821 W m^{-1}K^{-1}, $\lambda_u(w/c=0.3)=1.257$ W m^{-1}K^{-1}, and $\lambda_l(w/c=0.4)=0.837$ W m^{-1}K^{-1}, $\lambda_u(w/c=0.4)=1.164$ W m^{-1}K^{-1}. Deviation of the average calculated thermal conductivity (3K-HS) from the experimental results (Table 4) is −0.021 W m^{-1}K^{-1} for $w/c=0.3$, and +0.020 W m^{-1}K^{-1} for $w/c=0.4$. Calculated values for thermal conductivity of the fresh cement pastes based on the 2K-HS model are $\lambda_l(w/c=0.3)=1.026$ W m^{-1}K^{-1}, $\lambda_u(w/c=0.3)=1.086$ W m^{-1}K^{-1}, and $\lambda_l(w/c=0.4)=0.954$ W m^{-1}K^{-1}, $\lambda_u(w/c=0.4)=1.010$ W m^{-1}K^{-1}. Deviation of the average calculated thermal conductivity (2K-HS) from the experimental results (Table 4) is −0.004 W m^{-1}K^{-1} for $w/c=0.3$, and +0.002 W m^{-1}K^{-1} for $w/c=0.4$.

From the results it follows that the 2K-HS model of the fresh cement pastes makes more accurate estimates of the thermal conductivity with the lower differences between the two HS bounds than the 3K-HS model. This can be attributed to the two orders of magnitude difference between thermal conductivity of the air component and the cement or water components. Greater differences in components thermal conductivities result in wider margins of the HS model. Furthermore the influence of the entrapped air content of fresh cement pastes is hard to predict due to its non-uniform distribution. The 2K-HS model provides a reasonable means to estimate thermal conductivities of the 'consolidated' fresh cement paste composite with a different water volume fraction [12]. As the air component has a high impact on thermal conductivity of the cement paste composite one must be careful in considering its influence. For the higher entrapped air contents and/or entrained air by using admixtures, and to account for its change with w/c ratio, the 3K-HS model should be preferred.

4.2.3. Heat capacity

Specific heat capacities shown in Table 4, are calculated from measured densities, thermal conductivities and diffusivities by applying Eq. (1). According to a propagation of error analysis the estimated uncertainty in the calculated heat capacity is 4% with a 95% confidence level.

The heat capacity for fresh cement pastes was modeled by applying the law of mixtures:

$$c_p(\text{PasteFresh}) = c_p(H)\,m(H) + c_p(C)m(C) \tag{7}$$

where $m(H)$ and $m(C)$ are the mass fraction of water and cement powder in the fresh paste, respectively. Heat capacity of water is well known [34] (4.184 J/(g K) at 20 °C). A value of 0.78 J/(g K) is estimated for cement powder, based on the literature values for CA [35]. Applying Eq. (7) calculates a fresh cement pastes heat capacity to be 1.75 J/(g K) for $w/c=0.4$ and 1.56 J/(g K) for $w/c=0.3$. Comparison of this modeled values to a values provided in Table 1 for $w/c=0.4$ and 0.3 gave a deviations of 3.8% and 2.8%, respectively. These deviations are within an estimated uncertainty of obtained heat capacity based on experimental results and show good applicability of the law of mixture for predicting the heat capacity of fresh cement pastes.

For hydrated material obtained by hydration at 15 °C the results indicate a slight increase of the heat capacity, which is below the precision level of determination. Hydration at 30 °C gives hydrated material with 7% and 8% lower heat capacities from the fresh pastes $w/c=0.4$ and 0.3, respectively. Fully converted material has 15% lower value of heat capacity from the fresh pastes. These interesting results point to a relatively high heat capacity for hydration products at 15 °C, nominally CAH_{10}. It should be emphasized that this product contains 6 molecules of water and exhibits low crystalline level. Anomaly high heat capacity for bulk water is attributed to the energy used for the bending and breaking of hydrogen bonds. Hence, hydration at higher temperatures makes a pronounced lowering of heat capacity during hydration due to a more chemically and physically bound water within the hydration products. At higher temperatures the hydration products contain more crystalline water (OH^-), higher crystalline level, and the hydration degree is higher due to the lower stoichiometric water requirement of the higher temperature hydration reactions [3,36,37].

4.3. Evolution of thermal properties

During the cement setting and hardening, microstructure of material and amounts of individual phases (hydraulic cement minerals, water and formed hydrates) are changing continuously.

Measurements of thermal properties evolution during hydration are quite a challenge, especially for CAC, because the real temperature evolution is a superposition of the Joule heat in the hot wire and the heat generation due to hydration reactions. Simple corrections of subtracting the temperature increase due to hydration heat from the wire temperature may lead to serious error due to different (hard to predict) temperature field caused by a temperature sensitivity of hydration reactions. To minimize this effect temperature gradients caused both by hydration reaction and hot wire should be as low as possible. Although a lot of effort was put in this work to obtain thermal conductivity at a point of maximal, i.e. constant rate of hydration, current configuration of test device and analysis method didn't result in satisfactory results. However, thermal diffusivities determined at a point of maximal (constant) rate of hydration was considered possible with the adapted experimental configuration. To minimize aforementioned effect, smaller specimens, $2R=26$ mm and lower temperature change, $\Delta T\sim 3$ K were used. Results of the heating and cooling tests on same specimens were within measuring precision. This validates that by the applied method the heat generation during maximal rate of hydration was not significantly influenced due to the temperature sensitivity of hydration reactions.

In order to investigate the relative changes of thermal diffusivity during hydration the obtained experimental values, Table 4, are plotted against hydration degree, α Fig. 4. The degree of hydration is taken as the most suitable state parameter for describing the evolution of hydrating cement based materials properties [10]. The hydration degree at the maximal rate of hydration is estimated from the author's previous calorimetric results on the same cement [31]. The results indicated that 30% and 35% of the cumulative heat released in 30 h of hydration is released until the peak of the maximal rate of hydration, $w/c=0.4$ at $T=15$ and 30 °C, respectively. Degrees of hydration after 30 h are estimated based on results of reacted CA from previous studies [38]. One should bear in mind that accuracy of these final values is not considered as crucial for the intended investigation of thermal diffusivity evolution since the primary goal is the nature of the relative change. Therefore, to investigate the evolution of thermal diffusivity during hydration a degree of hydration is approximated as a degree of reacted CA. In the case of CAC, the most hydraulic phases are CA and $C_{12}A_7$, while C_2AS, C_2S and ferrite phase (C_4AF) are considered to have no significant reactivity at early ages (first 48 h) [3]. As $C_{12}A_7$ is present in much smaller quantities (~2–5%) than CA (40–60%) [3] and typically 70%–90% of the heat evolved is liberated in the first 24 h [4,31], estimation of a degree of hydration of early age hydration process based only on CA hydraulicity seems reasonable for the intended purpose. By this a constant ratio of amount of reacting CA and amount of other mineral components is assumed during first 30 h of hydration. Previous study on same cement [38] showed that for $w/c=0.4$ about 67% and 69% of CA has reacted in 30 h of hydration at 14 °C and 20 °C, respectively. In that work the QXRD analysis of investigated CAC gave the mass proportions of CA and $C_{12}A_7$

to be 41% and 4%, respectively. George [36] published results of hydration kinetics of CA by QXRD analysis of same class cement, $w/c = 0.4$, at temperatures between 20 and 70 °C. Although, he didn't document the quantities of CA and $C_{12}A_7$ in CAC, the results obtained at 20 °C indicate that about 68% of CA has reacted in 30 h, which is in good agreement with aforementioned value. The degree of hydration at 30 °C, $w/c = 0.4$, is approximated to be 80% [36].

Fig. 4 shows a linear change of thermal diffusivity as a function of hydration degree. For hydration at 15 °C (formation of mainly CAH_{10}) thermal diffusivity shows a linear decrease as a function of hydration degree (4% after 30 h of hydration). For hydration at 30 °C results point out to a linear increase of thermal diffusivity (5% after 30 h of hydration).

During hydration the volume fractions of unreacted cement and free water components decrease, while the fractions of formed hydration products and internal porosity (filled with air and water vapor in case of sealed conditions) increase. From the results obtained it is interesting to stress the following. As the volume fraction of the solids (components having the highest thermal conductivity) increases and the free water volume fraction decreases during hydration, the expected increase in the apparent thermal conductivity of cement paste is more than compensated by the formation of the internal porosity due to chemical shrinkage. In order to model the evolution of thermal properties during CAC hydration the volume fraction evolution of each phase has to be quantified. Unfortunately, in literature there is no such cement paste model for CAC hydration analog to Powers' model for PC hydration [17,39].

It is interesting to note why the thermal diffusivity changes in such a different way upon hydration at different temperatures, Fig. 4. During hydration the density remains essentially unchanged, i.e. there is no significant change of cement paste bulk volume. Furthermore, the thermal conductivity exhibits only marginal decrease. So according to Eq. (1) the main reason for the change in the thermal diffusivity during hydration is the change in the cement paste heat capacity (see discussion in Section 4.2.3).

4.4. Effect of temperature on thermal properties of hydrated material

4.4.1. Thermal diffusivity

As the moisture content is the key influencing parameter that determines thermal properties [16] this parameter was held constant for investigating the temperature dependence in this paper. Any mass exchange with the outside was prevented by sealing the mould and checked by mass measurements prior and after the tests.

The effect of temperature on thermal diffusivity was studied on specimens Conv70C $w/c = 0.4$ and 0.3 in temperature range 13–80 °C. Step inducement temperature difference (please see 3.4.1) were $\Delta T \sim 5$ K. Results shown in Fig. 5 are plotted against an average temperature of each testing inducement. The results on three repeated series of tests on $w/c = 0.4$ indicated that within the reproducibility of the measurements (±0.7% with 95% confidence), there is marginally decrease of thermal diffusivities of specimens with temperature. For a $w/c = 0.3$ a decrease of thermal diffusivity is observed in Fig. 5. In spite of a scatter in the data points a defined trend of thermal diffusivity with temperature is linearly fitted giving correlation coefficient $R^2 = 0.840$. The overall change for the investigated temperature range for $w/c = 0.3$ and 0.4 is 2% and 1.3%, respectively. The decrease is about the same magnitude as is the precision of the measurements. Low defined trend observed for $w/c = 0.4$ was also linearly fitted giving a correlation coefficient $R^2 = 0.470$. For neat pastes a decrease of about 2–6% in temperature range 25–80 °C was observed by Espinosa-Paredes [14].

4.4.2. Thermal conductivity

The effect of temperature on thermal conductivity was studied on the converted specimen Conv70C. Again, any mass exchange with the outside was prevented by sealing the mould and checked by mass measurements. The results shown in Fig. 6 indicate that thermal conductivities increase as the measurement temperature increases. Within the tested temperature range the results indicate an increase of thermal conductivity with temperature of 5.5% and 4% for $w/c = 0.3$ and 0.4, respectively. Espinosa-Paredes [14] also reported an increase of thermal conductivity of Mexican cementing systems used in geothermal well completion in the temperature range 28 to 200 °C. For neat pastes an increase of about 3–5% in temperature range 25–80 °C was observed from [14]. From Fig. 6 it can be seen that the influence of temperature is slightly more pronounced for the $w/c = 0.4$ in comparison to the $w/c = 0.3$.

4.4.3. Heat capacity

Considering the results in this paper of temperature dependence of thermal diffusivity and thermal conductivity, by applying Eq. (1) it follows that the specific heat increases by 7.5% and 5.3%, for the w/c of 0.3 and 0.4, respectively. This increase of specific heat with temperature is expected and agrees reasonably when referring to the literature of similar hydrated material [14,35]. For neat pastes an increase of about 2–6% in temperature range 25–80 °C could be observed from [14]. It is interesting to note that a lower increase for higher water content ($w/c = 0.4$) agrees with a fact of a decrease of water heat capacity with temperature [34].

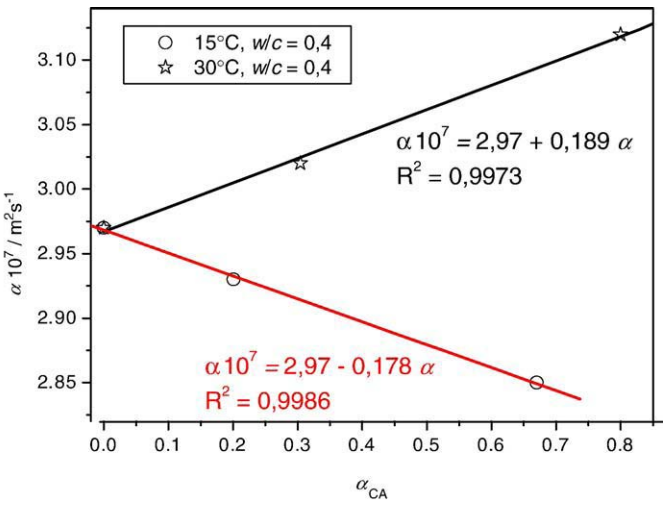

Fig. 4. Evolution of thermal diffusivity as a function of hydration degree.

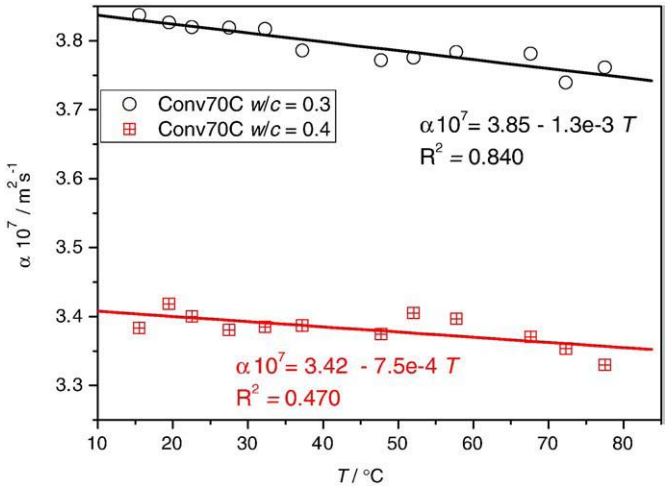

Fig. 5. Effect of temperature on thermal diffusivity for specimens Conv70C; $w/c = 0.4$ and 0.3.

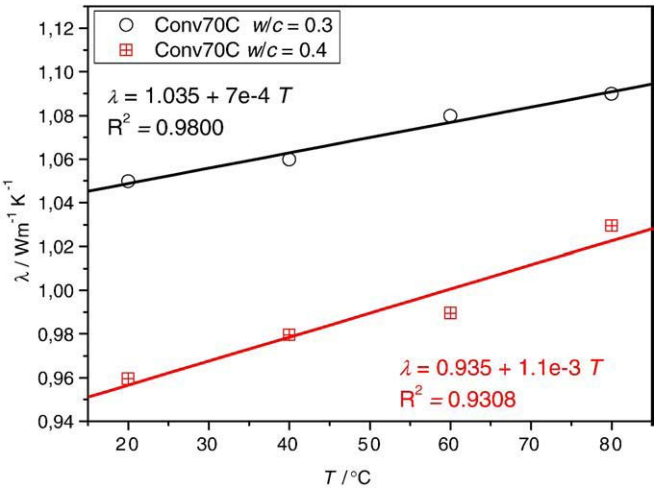

Fig. 6. Effect of temperature on thermal conductivity for specimens Conv70C; $w/c = 0.4$ and 0.3.

5. Conclusion

In this work a numerical approach for thermal diffusivity estimation was adopted for better accuracy and precision. The thermal conductivity was obtained by fitting the experimental results to a hot wire model by using previously obtained values for thermal diffusivity.

The thermal diffusivity and conductivity obtained on fresh cement paste for w/c of 0.3 are 11% and 8% higher, respectively, than for w/c of 0.4. For hydration at 15 °C (formation of mainly CAH_{10}) thermal diffusivity shows a linear decrease as a function of hydration degree (−4% after 30 h of hydration). For hydration at 30 °C results point out to a linear increase of thermal diffusivity (+5% after 30 h of hydration), while converted materials exhibited the highest values of thermal diffusivities. The results on converted material indicated that thermal conductivity increased 5.5% and 4% with an increase in temperature from 20 to 80 °C, while thermal diffusivities decreased 2% and 1.3% with temperature, for the w/c of 0.3 and 0.4, respectively.

The Hashin–Shtrikman boundary conditions and a simple law of mixtures can be used in estimating thermal conductivity and heat capacity, respectively, of fresh cement pastes.

Notation

Cement chemistry notation

A	Al_2O_3
C	CaO
F	Fe_2O_3
H	H_2O
S	SiO_2

Other used notation

$2R$	Inner diameter of specimen and cylindrical copper container
2K	Two component
a	Thermal diffusivity, $m^2\ s^{-1}$
A/D	Analog to digital
CAC	Calcium aluminate cement
c_p	Specific heat capacity, J/(kgK)
E_i	Exponential integral
HS	Hashin and Shtrickman
HW	Hot wire
l_w	Hot wire length, m
m	Mass fraction
P	Power of line (HW) heat source, W/m
PC	Portland cement
q_v	Volumetric heat generation, W/m^3
r	Radial dimension, m
R	Radius of cylindrical base of specimen, m
R^2	Correlation coefficient
r_w	Radius of hot wire, m
SD	Standard deviation, K
T	Temperature, ° C
t	Time, s
w/c	Water to cement mass ratio
z	Argument of exponential integral

Method

HW	Hot wire
QXRD	Quantitative X-ray diffraction

Greeks notation

α	Degree of hydration
γ	Euler's constant, $\gamma = 0.5772156649\ldots$
λ	Thermal conductivity, $W\ m^{-1}K^{-1}$
ρ	Density, $kg\ m^{-3}$
φ	Volume fraction

Subscripts

A	Air component
C	Cement powder component
H	Liquid water component
l	Lower HS bond
mp	Multi phase
u	Upper HS bond

Acknowledgements

The authors acknowledge support from the Croatian Ministry of Science, Education and Sports under project's no. 125-1252970-2983 “Development of Hydration Process Model”, and thank Mr. Jurica Alešković for building the computer-controlled hot wire apparatus, and Dr. Juraj Šipušić for a review of the manuscript.

References

[1] R.J. Mangabhai, F.P. Glasser (Eds.), Proc. Int. Conf. on CAC, Edinburgh, UK, 2001.
[2] R.J. Mangabhai (Ed.), Proc. Int. Conf. on CAC, Chapman and Hall, London, 1990.
[3] J. Bensted, Calcium Aluminate Cements, in: J. Bensted, P. Barnes (Eds.), Structure and Performance of Cements, 2end ed, 2002, pp. 114–138, London.
[4] C.M. George, Industrial aluminous cements, in: P. Barnes (Ed.), Structure and Performance of Cements, Applied Science, London, 1983, pp. 415–470.
[5] K.L. Scrivener, J.L. Cabiron, R. Letourneux, High-performance concretes from calcium aluminate cements, Cement and Concrete Research 29 (8) (1999) 1215–1223.
[6] N. Ukrainczyk, T. Matusinović, S. Kurajica, B. Zimmermann, J. Šipušić, Dehydration of a layered double hydroxide-C_2AH_8, Thermochimica Acta 464 (1) (2007) 7–15.
[7] T. Matusinović, N. Vrbos, J. Šipušić, Rapid setting and hardening calcium aluminate cement materials, Zement-Kalk-Gips International 5 (1) (2005) 72–79.
[8] L. Vozár, A computer-controlled apparatus for thermal conductivity measurement by the transient hot wire, Journal of Thermal Analysis 46 (2) (1996) 495–505.
[9] D.A. De Vries, The theory of heat and moisture transfer in porous media revisited, International Journal of Heat and Mass Transfer 30 (7) (1987) 1343–1350.
[10] G. De Schutter, L. Taerwe, Specific heat and thermal diffusivity of hardening concrete, Magazine of Concrete Research 47 (172) (1995) 203–208.
[11] G.D. Schutter, Thermal properties, in: A. Bentur (Ed.), Early Age Cracking in Cementitious Systems — RILEM Report 25, Technical committee 181-EAS: Early age shrinkage induced stresses and cracking in cementitious systems, 2003, pp. 121–125.
[12] D.P. Bentz, Transient plane source measurements of the thermal properties of hydrating cement pastes, Materials and Structures 40 (10) (2007) 1073–1080.
[13] E. Santoyo, A. Garcia, J.M. Morales, E. Contreras, G. Espinosa-Paredes, Effective thermal conductivity of Mexican geothermal cementing systems in the temperature range from 28 C to 200 C, Applied Thermal Engineering 21 (17) (2001) 1799–1812.
[14] G. Espinosa-Paredes, A. Garcia, E. Santoyo, E. Contreras, J.M. Morales, Thermal property measurement of Mexican geothermal cementing systems using an experimental technique based on the Jaeger method, Applied Thermal Engineering 22 (3) (2002) 279–294.
[15] W.N. Santos, Effect of moisture and porosity on the thermal conductivity of a conventional refractory concrete, International Journal of Heat and Mass Transfer 23 (5) (2003) 745–755.
[16] K.H. Kim, S.E. Jeon, J.K. Kim, S. Yang, An experimental study on thermal conductivity of concrete, Cement and Concrete Research 33 (3) (2003) 363–371.

[17] P. Mounanga, A. Khelidj, G. Bastian, Experimental study and modelling approaches for the thermal conductivity evolution of hydrating cement paste, Advances in Cement Research 16 (3) (2004) 95–103.
[18] H.S. Carslaw, J.C. Jaeger, Conduction of heat in solids, 2nd ed.Oxford University Press, London, 1959.
[19] N. Ukrainczyk, S. Kurajica, J. Šipušić, Thermophysical comparison of five commercial paraffin waxes as latent heat storage materials, Chemical and Biochemical Engineering Quarterly Journal, in press.
[20] A. Baïri, N. Laraqi, Diagrams for fast transient conduction in sphere and long cylinder subject to sudden and violent thermal effects on its surface, Applied Thermal Engineering 23 (11) (2003) 1373–1390.
[21] A. Baïri, N. Laraqi, J.M. Garcia de Maria, Determination of thermal diffusivity of foods using 1D Fourier cylindrical solution, Journal of Food Engineering 78 (2) (2007) 669–675.
[22] R.D. Skeel, M. Berzins, A method for the spatial discretization of parabolic equations, SIAM Journal on Scientific and Statistical Computing 11 (1) (1990) 1–32.
[23] L.F. Shampine, M.W. Reichelt, The MATLAB ODE suite, SIAM Journal on Scientific and Statistical Computing 18 (1) (1997) 1–22.
[24] K. Levenberg, A method for the solution of certain problems in least squares, Quarterly of Applied Mathematics 2 (1) (1944) 164–168.
[25] D.W. Marquardt, An algorithm for least-squares estimation of nonlinear parameters, SIAM Journal on Applied Mathematics 11 (2) (1963) 431–441.
[26] M.N. Ozisik, H.R.B. Orlande, Inverse Heat Transfer, Fundamentals and Applications, Taylor & Francis, New York and London, 2000. ISBN 1-56032-838-X
[27] N. Ukrainczyk, Thermal diffusivity estimation using numerical inverse solution for 1D heat conduction, International Journal of Heat and Mass Transfer 52 (2009) 5675–5681.
[28] G.C. Glatzmaier, W.F. Ramirez, , Simultaneous measurement of the thermal conductivity and thermal diffusivity of unconsolidated materials by the transient hot wire method, Review of Scientific Instruments 56 (7) (1985) 1394–1398.
[29] N. Ukrainczyk, J. Alešković, J. Šipušić, Determination of Thermal Conductivity by Transient Hot Wire Method, 14, International conference on Materials, Processes, Friction and Wear - MATRIB'09, Vela Luka, Croatia, June 2009, pp. 418–425, http://bib.irb.hr/datoteka/401667.HW_MATRIB09_Ukrainczyk.pdf.
[30] M.J. Assael, L. Karagiannidis, N. Malamataris, W.A. Wakeham, The transient hot-wire technique: a numerical approach, International Journal of Thermophysics 19 (2) (1998) 379–389.
[31] N. Ukrainczyk, J. Šipušić, P. Dabić, T. Matusinović, Microcalorimetric study on calcium aluminate cement hydration, 13, International conference on Materials, Processes, Friction and Wear — MATRIB'08, Vela Luka, Croatia, June, 2008, pp. 382–388, http://bib.irb.hr/datoteka/360481.Ukrainczyk.pdf.
[32] P.F. Hansen, J. Hansen, K. Hougaard, E.J. Pedersen, Thermal properties of hardening cement paste, Proceedings of RILEM International Conference on Concrete at Early Ages, RILEM, Paris, 1982, pp. 23–36.
[33] Z. Hashin, S. Shtrikman, A variational approach to the theory of the effective magnetic permeability of multiphase materials, Journal of Applied Physics 33 (10) (1962) 3125–3131.
[34] E.W. Lemmon, M.O. McLinden, D.G. Friend, Thermophysical properties of fluid systems, in: P.J. Linstrom, W.G. Mallard (Eds.), NIST Chemistry WebBook, NIST Standard Reference Database Number 69, National Institute of Standards and Technology, Gaithersburg MD, June 2005, p. 20899, http://webbook.nist.gov.
[35] V.I. Babushkin, G.N. Matvejev, O.P. Mčedlov-Petrosjan, Termodinamika Silikatov, Moskva, , 1972 in Russian.
[36] C.M. George, The hydration kinetics of refractory aluminous cements and their influence on concrete properties, Transactions and Journal of the British Society 79 (3) (1980) 82–90.
[37] C.M. George, Manufacture and Performance of Aluminous cement: a New Perspective, in [2], 181–207.
[38] N. Ukrainczyk, T. Matusinović, J. Šipušić, Microstructural model of calcium aluminate cement hydration, minerals to materials conference — M2M08 bridging the gap between minerals and materials, Central Metallurgical Research and Development Institute of Egypt, Cairo, 2008, http://bib.irb.hr/datoteka/377077.Ukrainczyk_m2m08.pdf.
[39] H.J.H. Brouwers, The work of Powers and Brownyard revisited: Part 1, Cement and Concrete Research 34 (9) (2004) 1697–1716.